

Single Unit Recordings in the Auditory Nerve of Congenitally Deaf White Cats: Morphological Correlates in the Cochlea and Cochlear Nucleus

D.K. RYUGO,^{1,2*} B.T. ROSENBAUM,¹ P.J. KIM,¹ J.K. NIPARKO,¹ AND A.A. SAADA¹

¹Center for Hearing Sciences, Department Otolaryngology–Head and Neck Surgery, Johns Hopkins University School of Medicine, Baltimore, Maryland 21205

²Department of Neuroscience, Johns Hopkins University School of Medicine, Baltimore, Maryland 21205

ABSTRACT

It is well known that experimentally induced cochlear damage produces structural, physiological, and biochemical alterations in neurons of the cochlear nucleus. In contrast, much less is known with respect to the naturally occurring cochlear pathology presented by congenital deafness. The present study attempts to relate organ of Corti structure and auditory nerve activity to the morphology of primary synaptic endings in the cochlear nucleus of congenitally deaf white cats. Our observations reveal that the amount of sound-evoked spike activity in auditory nerve fibers influences terminal morphology and synaptic structure in the anteroventral cochlear nucleus. Some white cats had no hearing. They exhibited severely reduced spontaneous activity and no sound-evoked activity in auditory nerve fibers. They had no recognizable organ of Corti, presented >90% loss of spiral ganglion cells, and displayed marked structural abnormalities of endbulbs of Held and their synapses. Other white cats had partial hearing and possessed auditory nerve fibers with a wide range of spontaneous activity but elevated sound-evoked thresholds (60–70 dB SPL). They also exhibited obvious abnormalities in the tectorial membrane, supporting cells, and Reissner's membrane throughout the cochlear duct and had complete inner and outer hair cell loss in the base. The spatial distribution of spiral ganglion cell loss correlated with the pattern of hair cell loss. Primary neurons of hearing-impaired cats displayed structural abnormalities of their endbulbs and synapses in the cochlear nucleus which were intermediate in form compared to normal and totally deaf cats. Changes in endbulb structure appear to correspond to relative levels of deafness. These data suggest that endbulb structure is significantly influenced by sound-evoked auditory nerve activity. *J. Comp. Neurol.* 397:532–548, 1998. © 1998 Wiley-Liss, Inc.

Indexing terms: organ of Corti structure; auditory nerve fibers; terminal morphology

Hereditary deafness in animals has been studied in different species including fox terriers (Wright, 1918), collie dogs (Lurie, 1948), white minks (Sugiura and Hilding, 1970), mice (Deol, 1970; Shone et al., 1991), Belgian canaries (Weisleder and Park, 1994), Dalmatians (Niparko and Finger, 1997), and congenitally deaf white cats (Mair, 1973; West and Harrison, 1973). All of these animals share characteristic features of pigment abnormalities that are associated with hearing loss. An autosomal dominant gene links white fur, heterochromia irides, and deafness in some but not all cats carrying the gene, and cochleosaccular degeneration has been demonstrated as the pathophysiologic event producing sensorineural hearing loss (Bosher and Hallpike, 1965; Bergsma and Brown, 1971). This

condition in the congenitally deaf white cat mimics the Scheibe deformity of humans and is thought to produce sensory degeneration that commences during the 1st week of life (Suga and Hattler, 1970; Mair, 1973).

Genetically programmed degeneration of cochlear hair cell receptors in deaf white cats provides a model in which

Grant sponsor: National Institute of Deafness and Other Communication Disorders, National Institutes of Health; Grant number: 5 RO1 DC00232.

*Correspondence to: David K. Ryugo, Center for Hearing Sciences, Traylor Research Building, Rm 510, Johns Hopkins Univ. School of Medicine, 720 Rutland Avenue, Baltimore, MD 21205. E-mail: dryugo@bme.jhu.edu

Received 20 August 1996; Revised 6 April 1998; Accepted 14 April 1998

to investigate transneuronal influences in the cochlear nucleus mediated by auditory nerve fibers. That is, cell changes in various centers in the central auditory pathway have provided evidence for transneuronal pathology. There is a marked but variable reduction in number of spiral ganglion neurons (Wilson and Kane, 1959; Rebillard et al., 1981a,b), and additional alterations are expressed higher in the auditory neuraxis to include the cochlear nucleus (West and Harrison, 1973; Larsen and Kirchhoff, 1992; Saada et al., 1996; Huchton et al., 1997) and superior olivary complex (Schwartz and Higa, 1982). Compared to normal-hearing cats, there is a 38–50% reduction in the size of spherical bushy cells in the anteroventral cochlear nucleus and a 31% reduction in the size of pyramidal cells in the dorsal cochlear nucleus (West and Harrison, 1973; Larsen and Kirchhoff, 1992; Saada et al., 1996). In the medial superior olive, cell size was reduced by roughly 14%, and the number of axosomatic synapses was reduced by approximately 35% (Schwartz and Higa, 1982). These changes are presumably mediated by loss of receptor cells in the cochlea which produces a cessation of spike activity in the auditory nerve. It is this loss of activity which appears to be one of the main variables underlying deafness-induced central pathologies (Lippe et al., 1980; Born and Rubel, 1985; Tucci et al., 1987; Rubel et al., 1990; Ryugo et al., 1997).

In the present study of congenitally deaf white cats, we hypothesized that single auditory nerve fibers would not only be unresponsive to acoustic stimulation but would also exhibit no spontaneous spike activity. Instead, we found some white cats with a family history of deafness to be hearing impaired (but not profoundly deaf), exhibiting spontaneous spike discharges as well as high-threshold, sound-evoked activity. The data separate "white cats" into two distinct groups. The previously reported deaf white cats (DWCs) are profoundly deaf, whereas a group of partially deaf white cats (pDWCs) possessed impaired yet functional hearing. Results are described in terms of the histopathological status of the cochleae and cochlear nuclei and the electrophysiological response properties of single auditory nerve fibers. We propose that definable changes in auditory nerve endings accompany congenital deafness and are mediated, at least in part, by afferent influences arising in the cochlea.

MATERIALS AND METHODS

Subjects

Two pigmented cats (a 3-kg male and a 1.8-kg female) with normal hearing but of unknown age were obtained from a licensed vendor. Six white cats with a family history of deafness, white fur, and anomalous iris pigmentation were purchased from Bowman Gray School of Medicine (Table 1). The white cats consisted of two males and four females, spanning three generations. These cats were a product of inbreeding, but only one was the direct offspring of another (DWC-1 is the offspring of pDWC-2). All cats appeared healthy in that they exhibited normal movements and respiration, were free of mange, and had clear eyes. All external ear canals were examined with an otoscope to verify that the tympanic membranes were intact and normal in appearance and that there were no ear mites or external ear infections. All animal procedures were used in accordance with the guidelines established by

TABLE 1. Deaf White Cats

Cat	Age	Sex	Wt. (lbs)	ABR threshold at 3 months		Single unit thresholds	
				Left ear	Right ear	Left ear	Right ear
DWC 1	5 yrs, 50 wks	M	7.25	>105 dB	>105 dB	>100 dB	—
DWC 2	7 yrs, 11 mos	F	6.0	25 dB	25 dB	—	62 dB
DWC 3	6 yrs, 5 mos	F	9.0	>105 dB	>105 dB	—	>100 dB
DWC 4	8 yrs, 2 wks	F	7.1	55 dB	>105 dB	71 dB	—
DWC 5	12 yrs, 2 mos	F	5.5	95 dB	95 dB	—	>100 dB
DWC 6	6 yrs, 5 mos	M	10	>105 dB	>105 dB	—	—

¹ABR threshold data courtesy of J. Ryu (personal communication).

the NIH and with the approval of the Animal Care and Use Committee of the Johns Hopkins University School of Medicine.

Animal preparation

Cats were anesthetized by using IM injections of ketamine hydrochloride (25 mg/kg) and xylazine hydrochloride (0.5 mg/kg), followed by IP injections (0.4 cc/kg body weight) of diallyl barbituric acid (100 mg/ml) in a solution containing urethane (400 mg/ml) and ethylurea (400 mg/ml). Atropine was also given to reduce secretions (0.05 mg/kg). Once the animals were areflexic to paw pinches, a tracheotomy was performed, the cat was placed in a head holder, and the soft tissue covering the skull was removed. The posterior fossa was opened with rongeurs, dura reflected over the cerebellum, and the cerebellum retracted to expose the auditory nerve as it passed from the internal auditory meatus. Recording micropipettes were placed into the auditory nerve under direct microscopic control, where click thresholds and single units were isolated and recorded by using routine electrophysiologic methods (e.g., Ryugo and May, 1993). Recordings were made from one side only.

We used standard intracellular recording micropipettes and associated criteria in order to be certain that we actually contacted a single fiber (Fekete et al., 1984; Ryugo et al., 1996). We inferred that contact with an auditory nerve fiber was made when a sudden drop in the DC potential, usually -20 to -30 mV, was observed and recorded on a chart recorder (Gould 220). A shift of greater than -50 mV was ignored. We know from experience that large DC shifts are never associated with evoked responses to acoustic stimulation and never result in the recovery of an intracellularly labeled auditory nerve fiber. Whenever possible, a threshold tuning curve and a 10-second period of spontaneous discharge rate (SR) were obtained. An automated tuning curve maker (Lieberman, 1982) defined the unit response area with respect to stimulus frequency and stimulus level, where threshold criterion was set at an evoked rate increase of 10 spikes/sec. The tip of the tuning curve determined fiber characteristic frequency (CF, the pure tone frequency to which the unit was most sensitive). SR was defined as spike activity (spikes/sec) in the absence of sound controlled by the experimenter. The sharpness of each tuning curve tip was assessed by using the Q_{10} value, where fiber CF is divided by the width of the tuning curve 10 dB above the tip (Kiang et al., 1965). Recording micropipettes had impedances of 24–34 M Ω and were filled with a solution of 10% horseradish peroxidase (HRP) in 0.05 M Tris buffer (pH 7.3) containing 0.15 M KCl.

Our intracellular contact time was typically less than 5 minutes, sufficient for a tuning curve and sample of SR but insufficient for intracellular labeling. Under normal conditions, we pass 4 nA of positive current for at least 10 minutes after characterizing the fiber if we expect to recover it by using standard HRP histochemical methods. We attempted numerous intracellular injections, but the injection times were so brief that we could not expect to recover any individually labeled fiber. Consequently, at the end of each recording session extracellular injections were made into the nerve by using micropipettes (inside tip diameter, 40 μm) filled with 30% HRP. HRP was ejected by passing 5 μA of positive current (7 seconds on, 7 seconds off) for 5 minutes.

Histology

Approximately 24 hours after HRP injections, each cat was administered a lethal dose of sodium pentobarbital and perfused through the heart with 0.1 M phosphate-buffered saline (pH 7.6) containing 0.5% sodium nitrite, followed by 1.5 liters of 0.1 M phosphate-buffered fixative (pH 7.6) containing 2% glutaraldehyde and 2% paraformaldehyde. Each cochlea was then exposed, and fixative was slowly pumped into the round window and passively drained out the oval window. The cochleae were left overnight at 5°C in the same fixative solution and dissected out of the skull the following morning. Cochleae were decalcified for 2 or more weeks in 0.1 M ethylenediamine-tetra-acetic acid (EDTA) with 1% glutaraldehyde, embedded in a gelatin-albumin block, and sectioned on a Vibratome. Cochlear sections were oriented in a plane parallel to the modiolus, cut at a thickness of 50 μm and collected in serial order, mounted on gelatin-chrom alum-coated (subbed) slides, air-dried overnight, stained with 0.5% cresyl violet, dehydrated in ascending concentrations of ethanol, cleared in xylenes, and coverslipped with Permount.

Following vascular perfusion, each brain was postfixed overnight in fresh fixative. The next morning, the brainstem along with the cochlear nuclei were removed from the skull and embedded in a gelatin-albumin mixture hardened with glutaraldehyde. Sections were cut at a thickness of 50 μm on a Vibratome, collected in serial order in 0.1 M phosphate buffer, washed in the same buffer several times, and kept refrigerated at 4°C overnight. Sections were incubated for 60 minutes in phosphate-buffered 0.05% 3,3'-diaminobenzidine (DAB, grade II, Sigma, St. Louis, MO) activated with 0.01% hydrogen peroxide, washed several times with 0.1 M phosphate buffer, and alternate sections were mounted on subbed slides, stained with cresyl violet, and coverslipped with Permount.

The other set of sections was processed for ultrastructural analysis. Tissue was placed in 1% OsO_4 for 15 minutes, rinsed 5 \times 5 minutes in 0.1 M maleate buffer (pH 5.0), and stained in 1% uranyl acetate overnight. The following morning, the sections were again washed with 0.1 M maleate buffer, dehydrated in increasing concentrations of ethanol, soaked in propylene oxide, infiltrated with Epon, and embedded in fresh Epon between sheets of Aclar (Ted Pella, Inc., Redding, CA). Hardened sections were taped to labeled microscope slides for examination with a light microscope. Selected areas of interest in the anteroventral cochlear nucleus (AVCN) were drawn at 32 \times and 1,250 \times with the aid of a light microscope and drawing

tube, and particular attention was paid to terminal endbulbs and surrounding structures. Relevant labeled structures were identified and dissected from individual sections and re-embedded in BEEM[®] capsules for electron microscopic analysis. Ultrathin sections of approximately 75 nm thickness were collected in serial order on Formvar-coated grids, stained with 7% uranyl acetate, and viewed and photographed with a JEOL 100CX electron microscope. Total magnification for ultrastructural analysis was 56,000 \times . Because each ultrathin section represents a thin slice through each endbulb, only parts of the labeled endbulb can appear in any section and are referred to as ending profiles.

Cochlear analysis

Every other section from each cochlea was drawn by using a light microscope and drawing tube. Drawings of each section were then aligned in sequential order with digital software (NIH Image, Version 1.61), and the organ of Corti and Rosenthal's canal were outlined (Photoshop v.3.0, Adobe Systems Inc., Mountain View, CA). The resulting stack was rendered into a three-dimensional image (Voxblast, Vaytek Inc., Fairfield, IA), which could then be rotated and viewed from any arbitrary plane (Fig. 1A). For our purposes, each cochlea was rotated so that it was viewed down the modiolar axis (Fig. 1B).

The length of each organ of Corti and Rosenthal's canal was measured from the reconstructed cochleae (Fig. 1B) with computer-aided planimetry (SigmaScan, Jandel Scientific, San Rafael, CA), and each structure was divided into 20 segments of equal length for determination of spiral ganglion cell density and hair cell integrity. Ganglion cell density was measured in two ways: For normal-hearing or partially deaf ears, two consecutive sections at a 5% interval were selected, and all spiral ganglion cells in the relevant cross-section of the canal were drawn with the aid of a light microscope and drawing tube at a total magnification of 500 \times . Ganglion cell density was determined by dividing the count by the cross-sectional canal volume (canal area multiplied by section thickness). For comparison, a box 100 μm to a side was placed over the middle of the canal. Every ganglion cell whose nucleus touched upon or was contained within the box was counted, and the density was calculated. Only cells exhibiting a clear nucleus and well-defined nucleolus were included in the sample. Both sampling methods produced statistically identical results when applied to Rosenthal's canal of normal cats, and these data were consistent with those previously reported (Keithley and Schreiber, 1987).

In the deaf ears, there was an irregular distribution of spiral ganglion cells in Rosenthal's canal, so the box method could not be used. Consequently, all ganglion cells exhibiting a clear nucleus and well-defined nucleolus were counted for the entire cochlea. Density was computed by dividing the number of cells by the volume of the canal at 5% intervals by using consecutive sections. All counts for all cochleae were adjusted according to methods yielding an unbiased estimate (Abercrombie, 1946).

The analysis of hair cells was conducted by using light microscopy (100 \times oil immersion objective, NA 1.25). Guided by the interval map of Rosenthal's canal (Fig. 1B), we determined the presence or absence of hair cells in their respective rows. Our material was not adequate for analysis of the condition of the stereocilia. In order to correlate

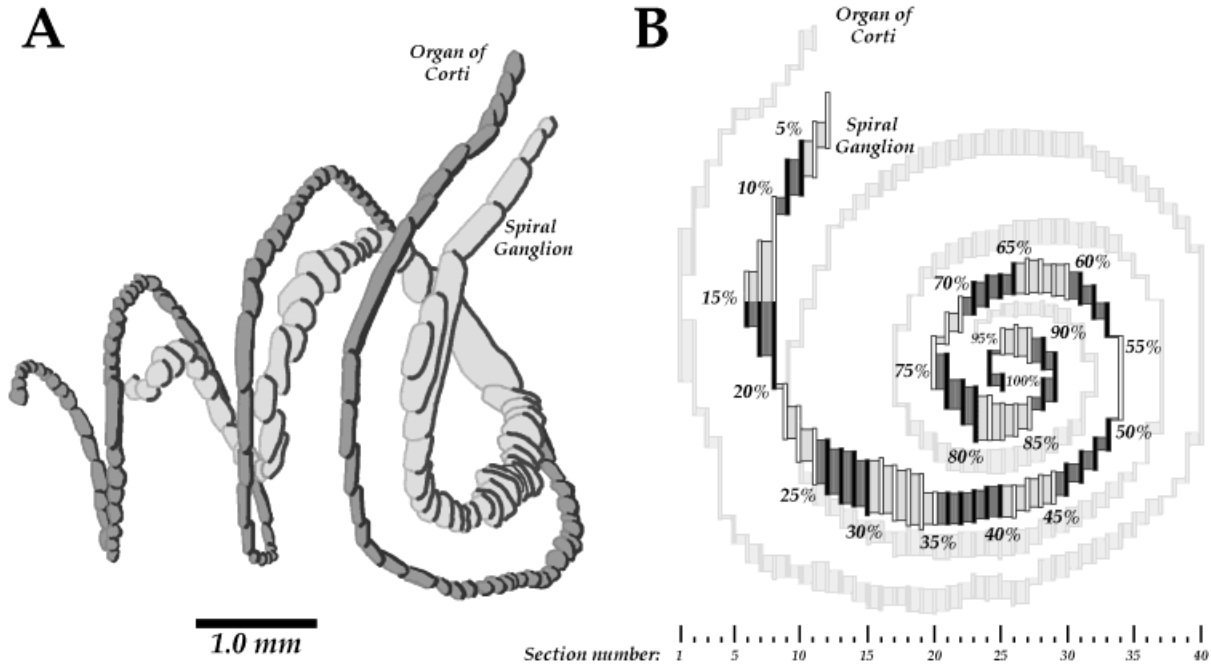


Fig. 1. Reconstructed organ of Corti and Rosenthal's canal, illustrating where hair cell analysis and spiral ganglion cell counts were conducted. **A:** Side view of computer-aided reconstruction from histologic sections illustrating the organ of Corti (dark shading) and Rosenthal's canal (housing the spiral ganglion, light shading). **B:** Apical

view of this reconstruction which was rotated to be seen down its modiolar axis. Each structure was divided into 20 segments of equal length so that analysis could be conducted in 5% intervals along the length. This procedure facilitated the mapping of cochlear location to histological sections.

electrophysiological frequency data with cochlear and cochlear nucleus structure, we utilized published frequency maps for the organ of Corti (Liberman, 1982), Rosenthal's canal (Keithley and Schreiber, 1987), and the cochlear nucleus (Bourk et al., 1981; Ryugo and May, 1993).

Endbulb analysis

All endbulbs were sampled from the 2–12 kHz region of the anteroventral cochlear nucleus. HRP-labeled endbulbs were drawn by using a light microscope and drawing tube (100× oil immersion objective, NA 1.25). With respect to the partially deaf white cats, a total of 31 endbulbs were sufficiently stained to be recovered from pDWC-2, and only ten were recovered from pDWC-4. From the completely deaf white cats, 32 endbulbs were recovered from DWC-6; fractal data from an additional 20 endbulbs of DWC-6 were included in this report which have been reported previously (Ryugo et al., 1997). A total of 184 endbulbs were analyzed from normal cats, of which 67 were part of a previous report (Ryugo et al., 1997). The silhouettes of all reconstructed endbulbs were digitized, the silhouette area calculated with NIH Image software, and the fractal dimension computed (Smith et al., 1989; Porter et al., 1991). Fractal geometry, which has been successfully applied as a quantitative descriptor of the complexity of natural structures (Mandelbrot, 1982), was used to assess endbulb complexity (Ryugo et al., 1997). We applied the box counting technique (Fractal Dimension Calculator, v1.5), where a grid of squares having 11 different sizes (s) is placed over the outline of the endbulb, and for each size, the number of squares N(s) that contain part of the endbulb is counted. The fractal dimension D is given by the

slope of the linear portion of the graph where log[N(s)] is plotted against log(1/s), derived from the relationship:

$$\log [N(s)] = D \log (1/s)$$

Because there is no preferred origin for the boxes with respect to the pixels in the image, multiple measures N(s) were computed from nine different box origins, and the graphed value of N(s) is the average from the different origins. Fractal values range between 1 and 2, and because the fractal index is represented on a logarithmic scale, each increase of 0.1 in the fractal dimension represents a doubling in endbulb complexity (Porter et al., 1991).

Ending profiles and postsynaptic densities (PSDs) were serially reconstructed from electron micrographs. Consecutive sections were aligned using NIH Image, and the resulting "stack" was rendered into a three-dimensional image and then rotated into optimal position and viewed. The reconstructed PSDs were best appreciated when viewed en face and were analyzed as they resided in the postsynaptic membrane. Absolute individual sizes could not be determined for every PSD because many continued further into unexamined sections. Section thickness was estimated by using standard interference reflection colors as the sections floated in the knife trough. The sections were silver in color, more gray than gold, and we estimate their thickness at 75 nm. This value is consistent with our reconstructions, because 14 sections, when rotated 90° and viewed en face, spanned slightly less than 1 μm as determined by a calibration grid, and 15 sections slightly exceeded 1 μm.

Silhouette area was used to represent the size of endbulbs and spherical bushy cells. Means (± standard devia-

TABLE 2. Single Unit Summary for DWCs

Cat	Total no. units	No. TCs	No. SR	SR range (s/s)	Mean SR \pm SD
DWC 1	25	0	25	0.0–58.2	19.4 \pm 33.8
DWC 2	99	28	71	0.2–100.8	42.9 \pm 24.2
DWC 3	11	0	3	0.0–8.4	1.85 \pm 4.2
DWC 4	75	6	69	0.1–148.3	83.2 \pm 44.6
DWC 5	5	0	5	4.7–50.6	16.2 \pm 19.5
DWC 6	0	—	—	—	—

tions) were calculated, group comparisons were conducted using Student's t-test (two-tailed, unpaired), Mann-Whitney U-test, or ANOVA (Statview II, v1.04, Abacus Concepts, Inc., Berkeley, CA), and *P* values are provided where appropriate. Photographic negatives were digitized (Leafscan 45), the contrast and/or exposure was adjusted (if necessary), simulating standard darkroom techniques (Adobe Photoshop), and the files were printed in high-resolution format (Fuji Pictography 3000).

RESULTS

Physiological recordings

The pigmented cats exhibited normal tuning curve thresholds (Liberman, 1978). N_1 thresholds to clicks were below 5 dB SPL, and below 10 dB SPL to 100-msec pure tone bursts between 0.5 and 15 kHz. These pigmented cats also exhibited startle and orientation responses to hand-claps presented behind their head. In contrast, white cats with a family history of deafness exhibited no such behavioral responses to similar noises, and our working hypothesis was that these white cats were deaf. The white cats (presumably much older than the pigmented cats) had thicker cranial bones and more vascularized soft tissue than did the pigmented cats. As a result, the surgery was more difficult, there was more bleeding and edema, and significant brain pulsation was present. In one of the cats (DWC-6), edema and bleeding prevented the acquisition of single unit recordings although anatomical data were collected.

Because we anticipated that few if any auditory nerve fibers would be activated by sound, we approached the task of recording using intracellular techniques. In this way, contact with an auditory nerve fiber would be unambiguous on the basis of an abrupt, negative shift in the DC potential to around -30 mV. This sudden shift of the resting potential permitted us to infer the presence of primary fibers, even when the fiber was acoustically unresponsive (up to 120 dB SPL). Once the pipette penetrated the axon, the DC potential gradually moved toward 0 mV, typically within 3–5 minutes or sooner. During this period, however, we were able to collect 10 seconds of SR and execute the automated tuning curve program. These short "holding" times made it impossible to recover injected auditory nerve fibers because successful labeling requires 5–10 minutes of intracellular current injection. We were, however, able to collect data from a number of units. Our strategy was to record from as many units in the auditory nerve as possible while the animal maintained its N_1 threshold to clicks.

White cats displayed distinct abnormalities in the population of single unit responses compared to control cats. Three of the white cats exhibited no evoked single unit responses to sound, and limited spontaneous spike activity (Table 2). The sampling of units was based upon intracellular penetration, so we did not bias our results by searching for the presence of action potentials. It should be noted

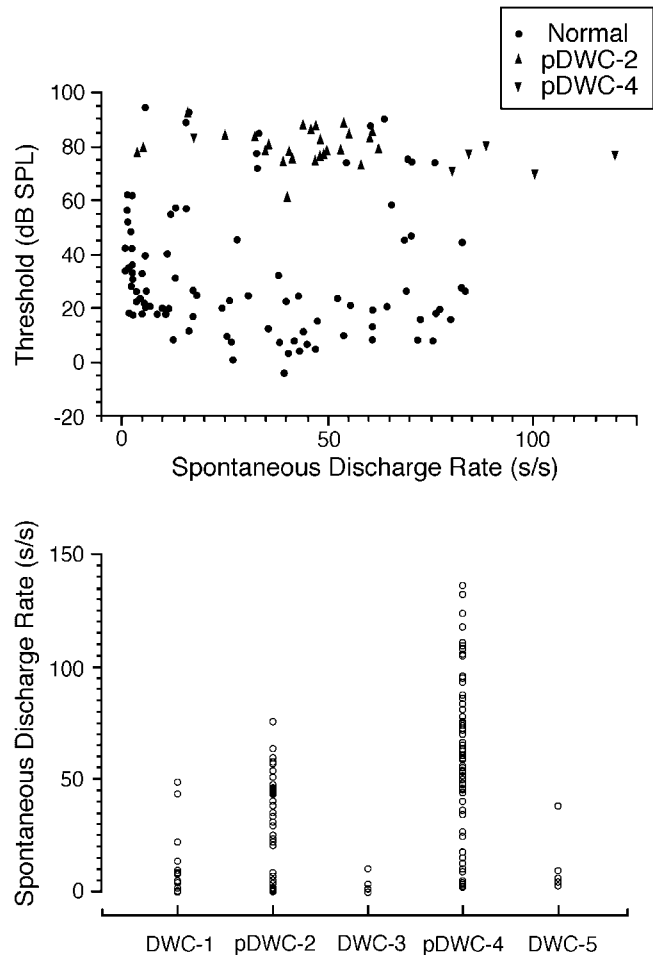


Fig. 2. **Top:** Scatter plot of spontaneous discharge rate (SR) versus threshold at characteristic frequency (CF) for two white cats with hearing loss and one cat with normal hearing. Note that for the white cats, single unit thresholds are high irrespective of SR values. **Bottom:** Plot of spontaneous discharge rates from units that were unresponsive to sound. Data are represented for each white cat separately.

that it was difficult to locate single fibers in the totally deaf cats. This difficulty is presumably due, at least in part, to ganglion cell loss. The auditory nerves were observed to be much thinner than normal during electrode placement; they were also highly subject to pulsation movement which further impeded fiber penetration. Although the number of units sampled per animal is small, the SR data were generally consistent in all three deaf cats (Fig. 2; Table 2).

In two other white cats, there were obvious evoked auditory responses, and tuning curves were collected (Fig. 3). Tuning curves from these partially deaf white cats (pDWC-2 and pDWC-4) were elevated in threshold, but nevertheless exhibited relatively sharp tips. The sharpness of each tip was assessed using the Q_{10} value, where Q_{10} magnitude was positively correlated with fiber CF in accordance with previously published reports (Kiang et al., 1965). Although both populations of fibers spanned the same frequency range (Fig. 4), they did not exhibit a normal frequency distribution, so they were compared using the Mann-Whitney U-test. Q_{10} values for the fibers of the

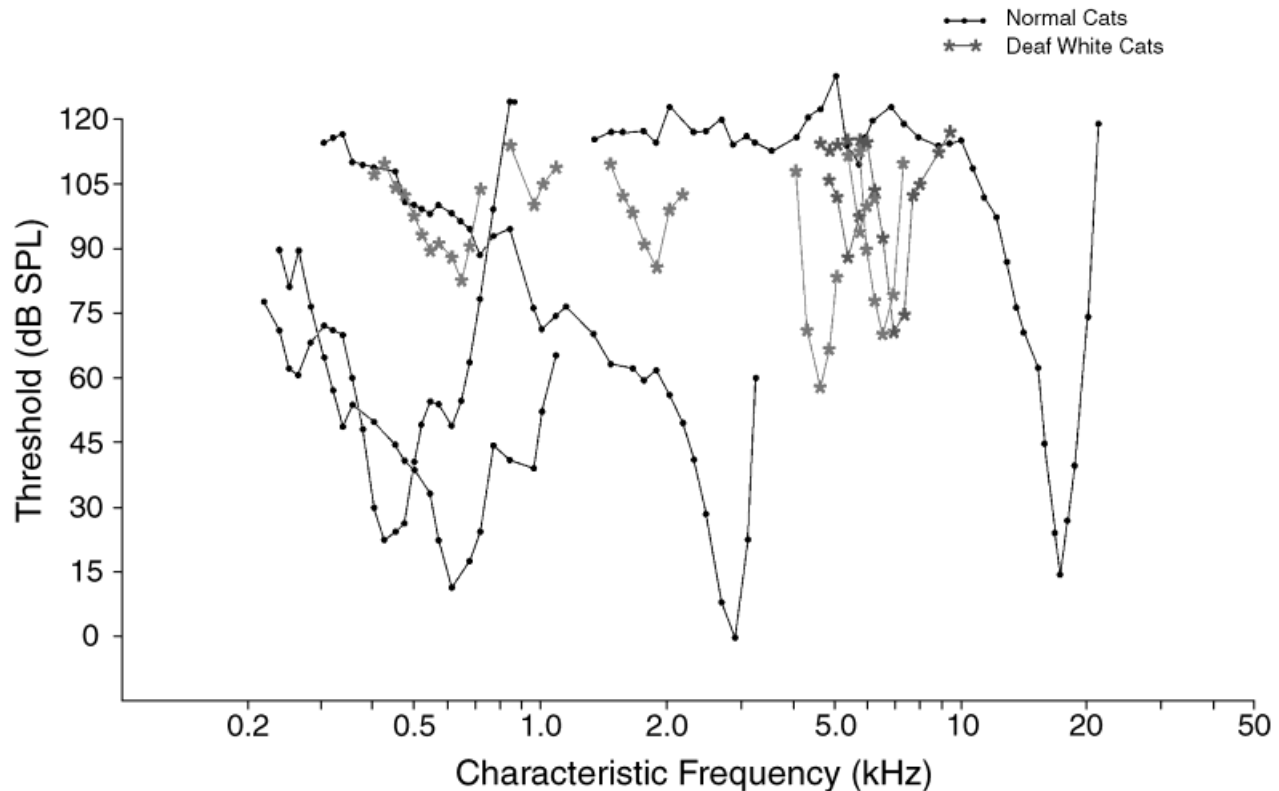


Fig. 3. Selected tuning curves from white cats with partial hearing (asterisks) compared to some from normal hearing cats (solid symbols). The tips of the tuning curves are V-shaped and equally sharp among both groups of cats, although those obtained from deaf cats exhibit elevated thresholds.

hearing-impaired white cats were not statistically different from those of normal-hearing cats ($P = 0.222$).

In the partially deaf cats, auditory nerve fibers exhibited spontaneous activity. Some units had resting levels of over 100 spikes/sec. In these white cats, the relationship between unit SR and unit CF threshold was abnormal. That is, in cats with "normal" hearing, high thresholds tend to be associated with low SR values (Kiang et al., 1965; Liberman, 1978). Acoustically responsive units in white cats, however, all exhibited high thresholds regardless of their SR values, and some acoustically unresponsive units had SR values greater than the highest values from normal-hearing cats. The upper quartile (range 112–150 spikes/sec) from pDWC-4 exceeded that of our normal cats (Fig. 2). Not only did single units in this cat exhibit higher rates of SR, but also there were proportionally more units at these higher rates. Six units had sound-evoked activity (CFs ranged from 2.7 to 7.1 kHz; thresholds >71 dB SPL) and 69 "deaf" units exhibited SR ranging from 0.1 to 148.3 spikes/sec. In pDWC-2, 28 units had sound-evoked responses (CFs ranged from 0.14–4.7 kHz; thresholds >60 dB SPL) and an additional 71 "deaf" units exhibited SR ranging from 0.2 to 100.8 spikes/sec (Fig. 2; Table 2). Regardless of the spontaneous activity levels, however, white cats as a group exhibited very low levels of evoked activity.

Cochlear morphology

The cochleae of DWC-1 and DWC-3 were not successfully processed. All cochleae of the other four white cats and two pigmented cats were examined with a light

microscope, and cochlear architecture was examined. The organs of Corti of white cats associated with elevated hearing thresholds (pDWC-2; pDWC-4) exhibited reliable and characteristic structural abnormalities (Fig. 5B) when compared to those of normal pigmented cats (Fig. 5A), and these features were distinctly different from those of the totally deaf cats. All inner and outer hair cells in the basal 20% of the cochlea were absent. Throughout the remaining length of the cochlea, a full complement of inner hair cells, rows 1 and 2 of outer hair cells, and the tunnel of Corti were present. Some outer hair cells of row 3 were missing, and the supporting cells of Hensen and Claudius were stacked abnormally high. In addition, Reissner's membrane bowed outward, and the tectorial membrane was unusually thin.

The cochleae of white cats associated with total deafness (DWC-4R; DWC-5 and DWC-6 bilaterally) exhibited marked structural abnormalities (Fig. 5C). The stria vascularis appeared severely reduced in thickness, Reissner's membrane was collapsed across the basilar membrane, and the tectorial membrane was degenerate and rolled up into the internal spiral sulcus. The collapse of Reissner's membrane obliterated the scala media, and the organ of Corti was so disrupted that inner hair cells (IHCs), outer hair cells (OHCs), supporting cells, and the tunnel of Corti could not be recognized.

Spiral ganglion cell density

The number of spiral ganglion cells in Rosenthal's canal was obviously different when comparing normal-hearing

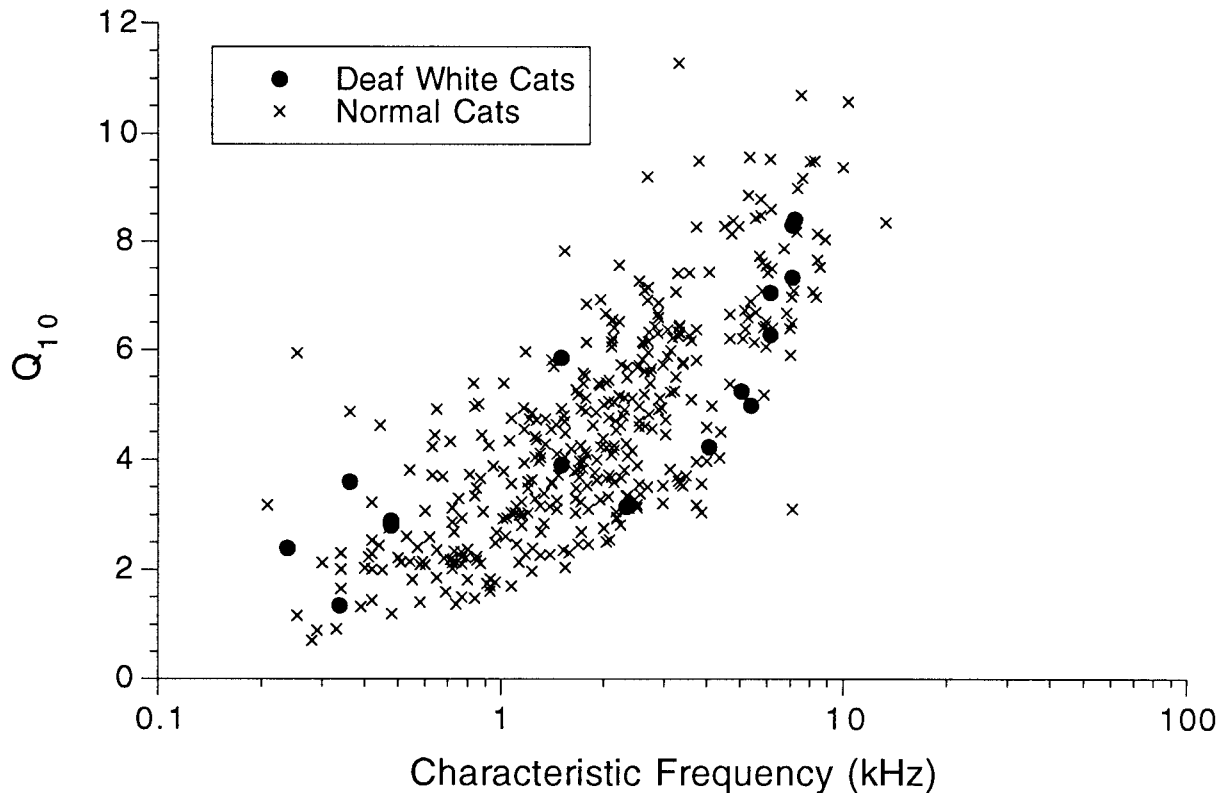


Fig. 4. Q_{10} values of tuning curves ($Q_{10} = \text{CF}$ divided by bandwidth at 10 dB re threshold) from white cats with partial hearing (solid circles) and normal-hearing cats (crosses). By this measure, the tips of tuning curves are equally sharp across both groups of cats. Some of the data from normal-hearing cats were provided by R.L. Miller, J.R. Schilling, K.R. Franck, and E.D. Young (personal communication).

cats to partially or totally deaf white cats (Fig. 6). Ganglion cell density was determined at 20 uniformly spaced intervals along the length of Rosenthal's canal. In comparison to cochleae with normal hearing (Fig. 6A), hearing-impaired cochleae had a somewhat reduced number of ganglion cells throughout Rosenthal's canal despite the presence of hair cells (Fig. 6C–E), and the totally deaf cochleae were severely depleted (Fig. 6B,F).

In the two pigmented cats, single unit thresholds were fairly typical across the audible frequency range (Fig. 7, top). The distributions of SR were also consistent with that reported for "normal" cats (Lieberman, 1978): They ranged from near zero to roughly 100 spikes/sec and exhibited an essentially bimodal distribution. In one of these pigmented cats, the single unit thresholds below 3 kHz were not as low as those reported for the 5- to 6-month-old chamber-raised cats of Lieberman (1978). It was clear, however, that the density of type I spiral ganglion neurons fell within the range of previously reported counts (Fig. 7, bottom).

In our sample of white cats, three cochleae were associated with elevated hearing thresholds, and five were associated with total deafness. Nevertheless, the nature of the cochlear histology corresponded with hearing thresholds (Fig. 8). Cochleae associated with elevated hearing thresholds exhibited total hair cell loss restricted to the basal 20–25% of the organ of Corti and corresponding loss of spiral ganglion cells that was greatest at the most basal region and whose severity diminished apically and reached normal values by the middle of the cochlea.

Two white cats had no organ of Corti (Fig. 5C; DWC-5, and DWC-6). They exhibited severe loss of spiral ganglion cells along the length of Rosenthal's canal (Fig. 6B,F). Ganglion cell density was determined for each cochlea at regular intervals along Rosenthal's canal (Fig. 9). There were 1,178 ganglion cells in the right cochlea and 1,016 in the left cochlea for DWC-5. There were 2,288 ganglion cells in the left cochlea and 2,894 ganglion cells in the right cochlea of DWC-6. The histologic verification of ganglion cell loss was consistent with the infrequent contact with single units during the physiological recording procedures, although given the lack of cochlear hair cells, it was surprising that any auditory nerve units had spontaneous spike activity.

Spiral ganglion cell size

One hundred ganglion cells from each turn of Rosenthal's canal from each cochlea were randomly selected from the density drawings and measured. Average somatic silhouette area (\pm SD) of spiral ganglion cells in pigmented cats was $197 \pm 45 \mu\text{m}^2$ in the apical turn (95th percentile), $198.8 \pm 38 \mu\text{m}^2$ in the middle turn (75th percentile), and $156.3 \pm 16 \mu\text{m}^2$ in the basal turn (20th percentile). In contrast, average somatic size for the DWCs was $180.5 \pm 39 \mu\text{m}^2$ in the apical turn, $171 \pm 32 \mu\text{m}^2$ in the middle turn, and $155.4 \pm 30 \mu\text{m}^2$ in the basal turn. There was no statistical difference in somatic silhouette area comparing pigmented ($n = 2$) and white cats ($n = 4$), or comparing

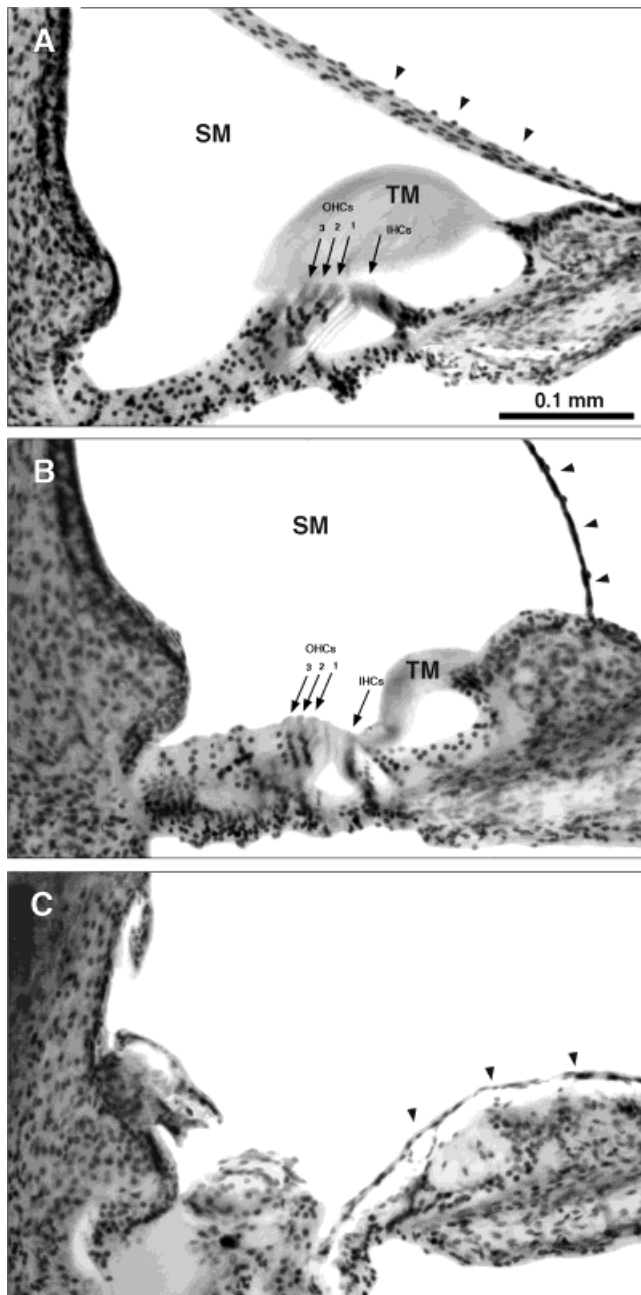


Fig. 5. Photomicrographs representative of the organ of Corti through the middle turn of the cochlea from three groups of cats. **A:** Normal-hearing, pigmented cat. The organ of Corti has an appearance consistent with that for normal cats. Arrows indicate apical surface of hair cells, where cylindrical cell bodies are evident above their nuclei. Arrowheads indicate Reissner's membrane. **B:** Partially hearing white cat (pDWC-2R), illustrating some of the cochlear abnormalities. Note the bulging Reissner's membrane (arrowheads), the unusually thin and short tectorial membrane (TM), and the missing outer hair cells of row 3 as revealed by the diminished number of nuclei. **C:** Totally deaf white cat (DWC-5) has no sign of hair cells, the tunnel of Corti has been obliterated, and the stria vascularis is abnormally thin. Reissner's membrane is indicated by arrowheads. IHC, inner hair cells; OHC, outer hair cells; SM, scala media; TM, tectorial membrane.

the totally deaf white cats ($n = 2$) to the partially deaf white cats ($n = 2$, ANOVA, $P = 0.392$).

Endbulbs of Held

HRP-stained endbulbs from profoundly deaf white cats are smaller than those of normal cats and exhibit less secondary and tertiary branching in their terminal arborizations (Ryugo et al., 1997). That is, the endbulbs exhibited simpler arborizations with fewer and thinner branches, fewer varicosities, and fewer terminal swellings. Previous research had revealed that endbulbs of the totally deaf white cats were severely reduced in their structural complexity (Ryugo et al., 1997). The issue addressed in this report relates to the morphology of endbulbs and synapses in white cats that are not totally deaf but instead exhibit elevated hearing thresholds. The hypothesis is that even a little hearing would serve to preserve some of the neural structure compared to that of animals with no hearing.

Normal-hearing cats

HRP-labeled auditory nerve fibers and their endbulbs were reliably distinguished with a light microscope due to the presence of intracellular reaction product that filled the axoplasm. Endbulbs from cats with normal hearing exhibit multiple branches stemming from a thick, gnarly trunk. Branches divide successively and give rise to numerous varicosities. Many fine, filamentous processes interconnect varicosities and branches, and terminal branches are marked by the presence of distinct swellings (Fig. 10A). We determined that the mean silhouette area of normal endbulbs is $417.3 \pm 181 \mu\text{m}^2$. Endbulb complexity was assessed with measurements of their fractal value (Ryugo et al., 1997). The fractal index of endbulbs ($n = 117$) from two normal-hearing cats is, on average, 1.440 ± 0.044 , a value very similar to what we had previously reported (Ryugo et al., 1996). The mean silhouette area of spherical bushy cell somata from normal-hearing cats is $623.8 \pm 38 \mu\text{m}^2$ ($n = 380$).

Partially deaf cats

Auditory nerve fibers originating from the middle turn of white cats with elevated thresholds (pDWC-2R and pDWC-4L) were labeled with HRP. These cats had auditory nerve fibers with spontaneous and evoked spike activity ranging from zero to greater than 200 spikes/sec. Although the number of labeled endbulbs from these cats was small ($n = 41$), a few of these endbulbs appeared relatively normal, whereas the majority had sparse arborizations with fewer than normal branches and component swellings (Fig. 10B). There were also an underdeveloped meshwork of interconnecting processes and diminished contact with the target spherical bushy cell. The mean silhouette area of the endbulbs was $193.81 \pm 49.3 \mu\text{m}^2$ and the mean fractal index of these endbulbs was 1.318 ± 0.066 , reflecting their smaller size and simpler structure. The silhouette area of the somata postsynaptic to these endbulbs was, on average, $378 \pm 70.7 \mu\text{m}^2$. Despite the generally high levels of spontaneous activity in this population of auditory nerve fibers, endbulbs and SBCs nevertheless exhibited definable abnormalities in structure.

Totally deaf cats

Endbulbs ($n = 52$) from the completely deaf cats (DWC-5 and DWC-6) were distinctly pathologic in their appearance. Labeled auditory nerve fibers arose from the upper

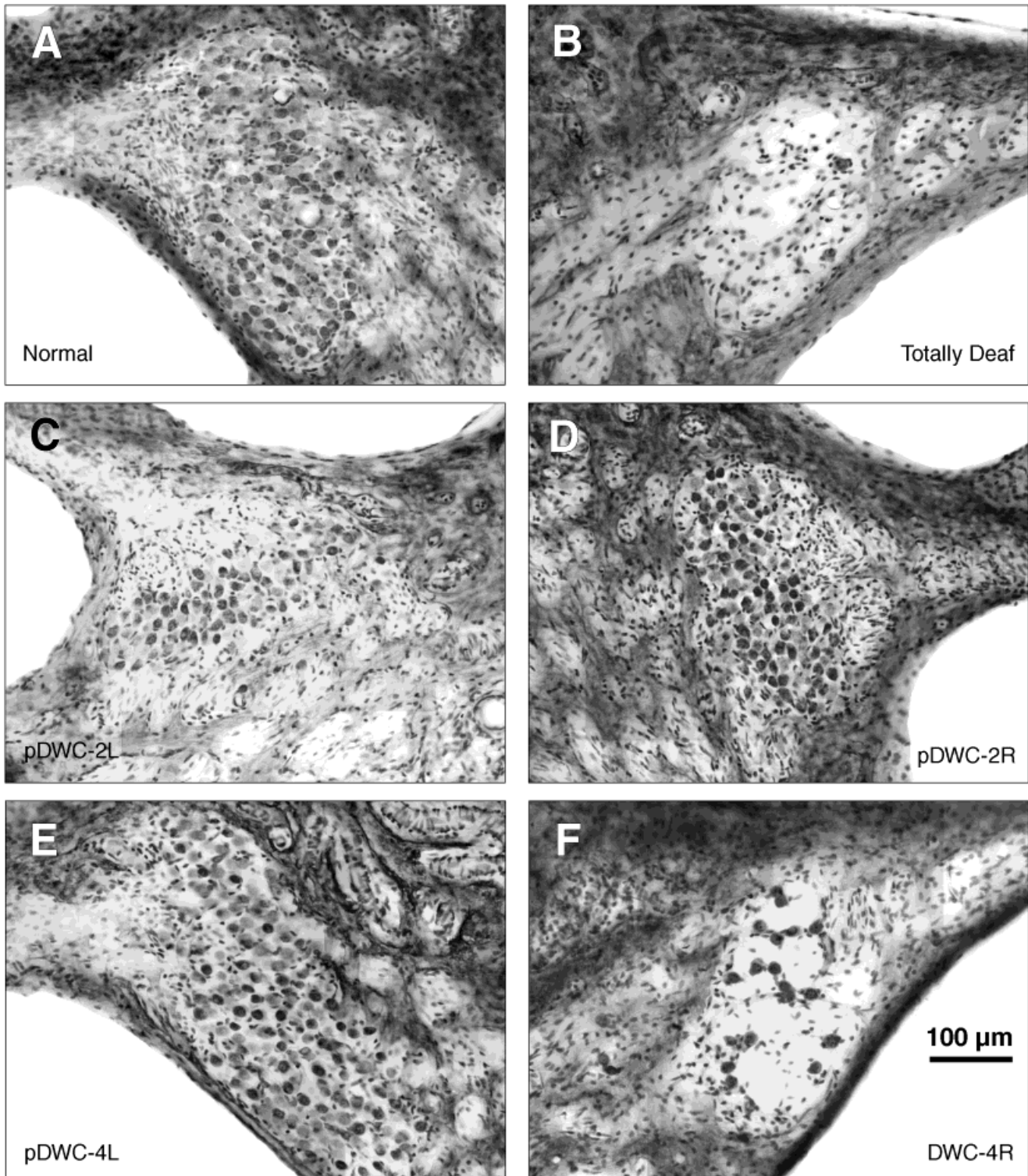


Fig. 6. Photomicrographs of Rosenthal's canal in the middle turn of the cochlea, representative of the three groups of cats. **A:** Normal-hearing, pigmented cat exhibiting its full complement of primary neurons. **B, F:** Rosenthal's canals from totally deaf ears (DWC-5L and DWC-4R, respectively) have lost more than 90% of their spiral

ganglion cells. **C-E:** Rosenthal's canals from ears with elevated thresholds (pDWC-2L, pDWC-2R, pDWC-4L, respectively) have lost few if any ganglion cells where the organ of Corti is intact, but up to 70% of the ganglion cells where there is complete loss of hair cells.

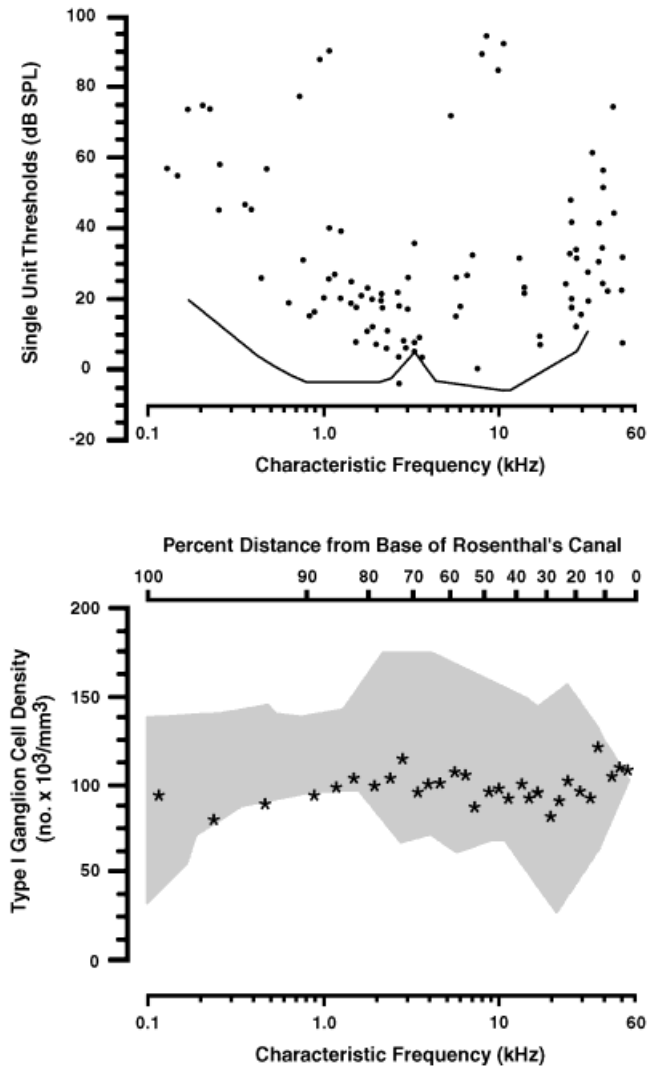


Fig. 7. Typical single unit data and ganglion cell counts from a normal-hearing, pigmented cat with an intact organ of Corti. **Top:** Scatter plot of single unit CFs and thresholds. The curve marks the best thresholds of single units from young cats raised in a relatively noise-free, sound-attenuated chamber (Lieberman, 1978). **Bottom:** Plot of spiral ganglion cell density as determined in 5% intervals and illustrated as percent distance from the base of Rosenthal's canal. The region in gray represents the envelope of previously reported ganglion cell counts from normal cats, and the frequency map was derived from single fiber labeling studies (Keithley and Schreiber, 1987).

middle turn of the cochleae from each cat. Arborizations were sparse with infrequent branches and were marked by few but generally large swellings (Fig. 10C). There was an obvious paucity of any kind of interconnecting meshwork. These features were reflected by their small silhouette area ($171.8 \pm 61 \mu\text{m}^2$) and a mean fractal index of 1.288 ± 0.055 , which signified low complexity among endbulbs. Similarly, the silhouette area of the postsynaptic spherical bushy cells was, on average, $358.6 \pm 73.1 \mu\text{m}^2$, a value statistically smaller than that of the partially deaf white cats. The mean fractal index and silhouette size for endbulbs of the three groups of cats (normal, partially deaf, and totally deaf), along with the somatic size of their

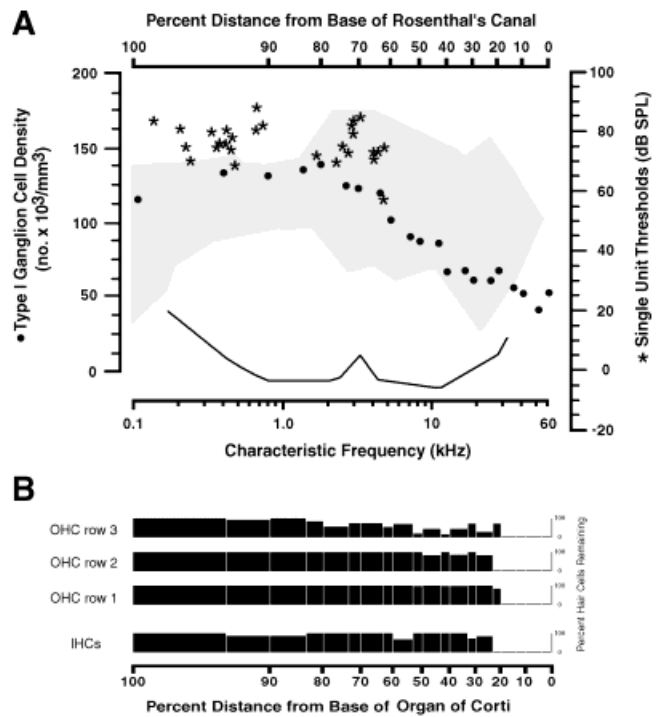


Fig. 8. Single unit data and ganglion cell counts from a partially hearing white cat (pDWC-2R). **A:** Scatter plot of single unit CFs and thresholds (asterisks) and ganglion cell density (solid symbols) as referenced to relative distance and frequency sensitivity. The curve marks the best thresholds of single units from young cats raised in a relatively noise-free, sound-attenuated chamber (Lieberman, 1978). Note that the thresholds of this white cat are elevated. The region in gray represents the envelope of previously reported ganglion cell counts from normal cats, and the frequency map was derived from single fiber labeling studies (Keithley and Schreiber, 1987). **B:** Plot of percent hair cells remaining as determined in 5% intervals and illustrated as percent distance from the base of Rosenthal's canal. All hair cells in the basal 20% are missing, with scattered loss of IHCs and row 3 OHCs. The loss of ganglion cells corresponds to the loss of cochlear hair cells.

associated postsynaptic spherical bushy cells, were statistically different for each group (ANOVA, $P < 0.05$).

Endbulb synapses

These alterations in endbulb appearance as an apparent reflection of relative hearing levels prompted us to examine endbulb synapses with an electron microscope (Table 3). Primary synapses from normal-hearing cats have been well described, so they will be only briefly mentioned for comparison purposes to those of the white cats. Transmitter release sites form around discrete postsynaptic densities, where the spherical bushy cell membrane bulges into the presynaptic endbulb (Fig. 11A). Clear, round synaptic vesicles are scattered throughout the endbulb cytoplasm ($n = 22$ endbulbs, 72.9 ± 29.6 vesicles/ μm^2), concentrating around the release sites. A normal endbulb may have up to 2,000 individual release sites (Ryugo et al., 1996) which are round to oval in shape and distributed uniformly against the postsynaptic bushy cell. In contrast, synapses from totally deaf white cats appear obviously different. Presynaptic vesicle density is distinctly reduced ($n = 36$ endbulbs, 46.1 ± 16.1 vesicles/ μm^2), and postsynaptic densities are thicker and considerably expanded (Fig. 11C).

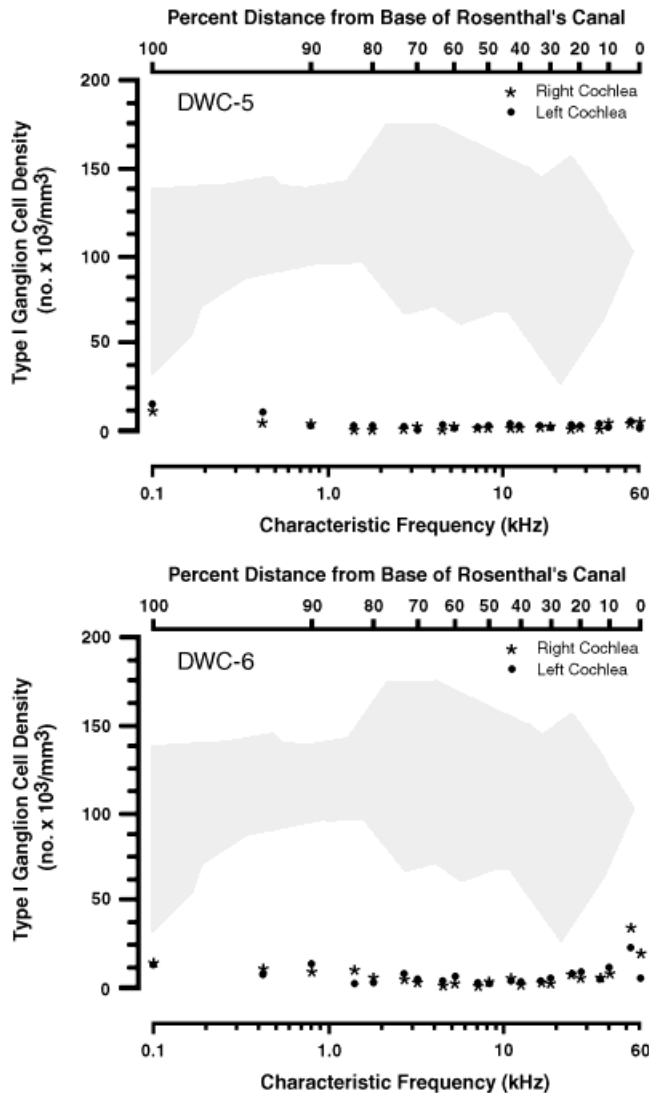


Fig. 9. Ganglion cell counts from two totally deaf white cats (DWC-5 and DWC-6). DWC-5 had a few spontaneously active auditory nerve fibers but no evoked responses; no single unit data were collected from DWC-6. The plot of spiral ganglion cell density reveals a relatively uniform cell loss throughout the length of Rosenthal's canal, presumably in response to the absence of an organ of Corti.

The synapses of partially deaf cats, however, were different from those of either the normal or totally deaf cats. The density of presynaptic vesicles was consistently elevated ($n = 29$ endbulbs, 92.9 ± 25.2 vesicles/ μm^2), yet the postsynaptic densities were not obviously different from those of normal-hearing cats (Fig. 11B). When the postsynaptic densities were reconstructed and examined en face, the difference between the totally deaf white cats versus hearing and partially hearing cats is revealed (Fig. 12). The mean surface area of postsynaptic densities for normal-hearing cats ($0.06 \pm 0.04 \mu\text{m}^2$) is smaller but does not reach statistical significance compared to that of partially deaf cats ($0.1 \pm 0.08 \mu\text{m}^2$), whereas that of the totally deaf white cats is very much larger than that of either normal or partially deaf cats ($0.34 \pm 0.37 \mu\text{m}^2$, $P < 0.05$, ANOVA).

DISCUSSION

In the present study, we correlated single unit population data to the corresponding morphology of the organ of Corti, spiral ganglion cells, and central auditory nerve terminations represented by endbulbs of Held. Four white cats were considered to be profoundly deaf because tones between 0.1 and 40 kHz and exceeding 100 dB SPL were incapable of evoking spike activity in the auditory nerve. Furthermore, there was little spontaneous activity in the auditory nerve fibers. These cats, deaf since at least 3 months of age on the basis of no auditory evoked responses, exhibited a collapse of Reissner's membrane onto the organ of Corti and a complete loss of inner and outer hair cells. Furthermore, there was greater than 90% loss of spiral ganglion cells. These anatomical observations are generally consistent with previously published data in the auditory periphery of deaf white cats (Mair, 1973; Schwartz and Higa, 1982). The present study extends basic anatomical descriptions of congenitally deaf cochleae in demonstrating that retained ganglion cells give rise to abnormal endbulbs of Held whose simple appearance was objectively confirmed by fractal analysis. These endings also exhibited pathologic synapses, characterized by reduced numbers of synaptic vesicles and greatly hypertrophied postsynaptic densities.

Two other white cats from the same family line were not totally deaf but were congenitally hearing impaired, especially for high frequencies. Their auditory nerve fibers exhibited single unit thresholds in excess of 60 dB SPL for tones below 10 kHz, and many units had spontaneous activity. Units between 10 and 40 kHz, however, were unresponsive to tones (exceeding 100 dB SPL). In these cats with more moderate physiological indices of hearing loss, there was a characteristic loss of hair cell receptors in the basal 20% of the organ of Corti with scattered loss of inner hair cells and row 3 outer hair cells throughout the remainder of the organ. Ganglion cell loss accompanied the hair cell loss and approached 50% in the most severely affected regions of the cochlear base. Ganglion cell density in Rosenthal's canal was otherwise seemingly normal. The cat with better hearing as evidenced by more units activated by sound had a greater density of ganglion cells. Those ganglion cells that remained gave rise to endbulb terminals that had an intermediate level of complexity compared to those of normal and totally deaf cats; furthermore, their endbulbs exhibited synapses with higher numbers of vesicles and slightly (but not statistically) larger postsynaptic densities. These data on the deaf white cats reveal a complex relationship between hearing levels and structural correlates, suggesting that the underlying source of the functional loss may be quite variable.

A seminal publication on deaf white cats (Mair, 1973) concluded that deafness begins with the progressive loss of hair cells initiated during the 1st postnatal week of life and continues throughout the 1st and 2nd years. The degenerative process follows a regular pattern, whereby change spreads in a sequential way along the cochlear duct from the upper half of the basal coil toward the apex. Secondary to hair cell loss was loss of primary neurons, and the general inference was that older animals suffered more severe deafness than did younger animals. In contrast to Mair's (1973) publication, Boshier and Hallpike (1965) reported that hair cell degeneration could occur simultaneously in all cochlear turns, and Bergsma and

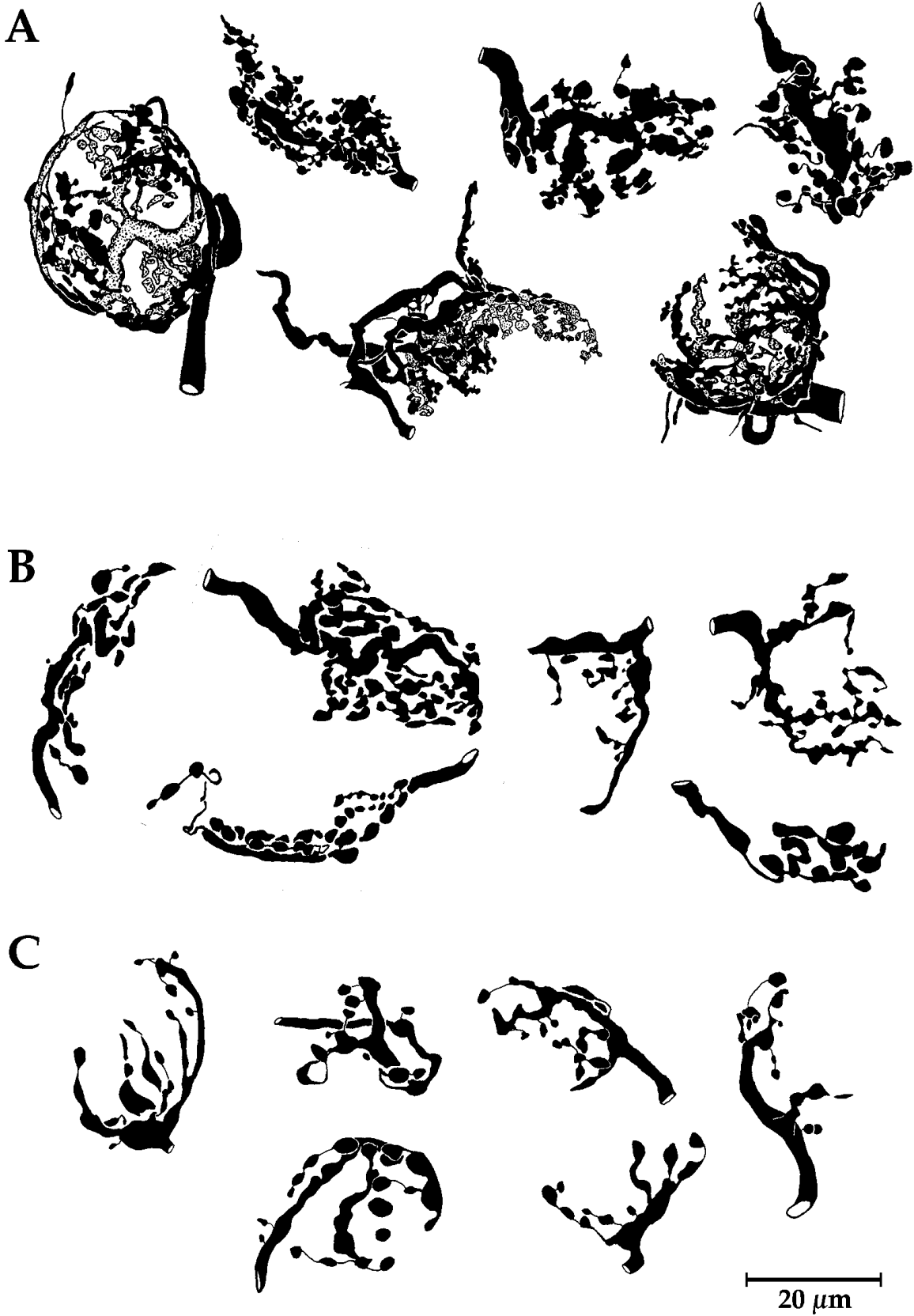


Fig. 10. Drawing tube reconstructions of endbulbs of Held. These reconstructions are representative of each respective population and span the range of endbulb appearance. **A:** Endbulbs from normal-hearing cats. These large, axosomatic endings emerge from the end of the myelinated auditory nerve fibers, branch once or several times, and then arborize profusely into smaller branches with en passant varicosities and terminal swellings. **B:** The endbulbs of partially hearing cats tend to have fewer branches but still exhibit a relatively

complex and delicate arborization. **C:** Endbulbs from totally deaf cats are clearly simpler in form, exhibiting prominent swellings but none of the fine delicate branching. The structural quality of the endbulbs clearly reflects the hearing status of the cats. Fractal analysis revealed that endbulb shape from normal-hearing cats is twice as complex as that of partially hearing cats, which in turn is twice as complex as that of totally deaf cats.

TABLE 3. Endbulb Morphometric Measurements Summary

Cat	EB area \pm SD (μm^2)	Fractal index \pm SD	SBC size \pm SD (μm^2)
Normal (n = 56)	417.3 \pm 181 (n = 184)	1.440 \pm 0.044 (n = 117)	623.8 \pm 38 (n = 380)
Partially deaf (n = 2)	193.8 \pm 49.3 (n = 41)	1.318 \pm 0.066 (n = 41)	378 \pm 70.7 (n = 200)
Deaf (n = 4)	171.8 \pm 61 (n = 52)	1.288 \pm 0.055 (n = 52)	358.6 \pm 73.1 (n = 400)

Brown (1971) reported that there could be normal regions of the organ of Corti in deaf white cats. Subsequently, reports surfaced which agreed that hereditary degeneration in the cochlea of white cats was not necessarily a regular process, and that in a few cases ganglion cell loss preceded cochlear degeneration (Pujol et al., 1977; Rebillard et al., 1981a,b). It should also be emphasized that the early work on the congenitally deaf white cats (e.g., Boshier and Hallpike, 1965; Bergsma and Brown, 1971; Mair, 1973) addressed deafness as an all-or-none phenomenon, occurring either unilaterally or bilaterally. The first hint of partial deafness in these white cats came in a brief statement about a cat with "poor hearing" on one side (Rebillard et al., 1976). Certainly some of the cats in our sample exhibit different degrees of hearing loss. Given variations in histopathology and hearing status across the populations of congenitally deaf white cats, it is apparent that the general class of deaf white cats is not homogeneous. We are reminded how important it is to track pedigree and/or age of the animal at the time studied.

Single unit activity

Based upon studies of acoustic trauma, neural tuning curves of primary auditory afferents reliably indicate the site of cochlear hair cell damage (Lieberman and Kiang, 1978; Lieberman and Dodds, 1984b; Kiang et al., 1986; Wang et al., 1997). Sharp tuning curve tips with elevated thresholds correlate with stereocilia damage of the inner hair cell and the first row of outer hair cells (Lieberman and Dodds, 1984b). These observations are mostly consistent with reports of auditory nerve fibers in chinchillas with carboplatin-induced inner hair cell loss, but not outer hair cell loss (Wang et al., 1997): Spontaneous discharge rates are reduced, tuning is still sharp, but thresholds are elevated. The tuning curves of the DWCs exhibited elevated thresholds with the preservation of sharp tips at characteristic frequency. The sharpness of the tuning curves as determined by Q_{10} values demonstrated that they were comparable to those of normal auditory nerve fibers. In white cats with elevated thresholds, there was a full complement of hair cells, but the tectorial membrane was abnormally thin and did not appear to reach the apical surface of the hair cells. This pathologic condition suggests, at least in part, that the stereocilia of the inner hair cells were not adequately stimulated in the presence of sound. We could not detect stereocilia disarray or damage with our histologic preparations, but the shape of the tuning curves in the hearing-impaired white cats is consistent with inner hair cell involvement. Because the features of cochlear pathology that we report here were systematically coupled to the separate groups of cats with different hearing abilities, we infer that the cochlear abnormalities were not fixation artifacts. In addition, cochlear tissue prepared by plastic-embedding techniques are consistent with these current findings (unpublished observations).

Spontaneous activity in auditory nerve fibers reflects the status of the cochlea. In normal-hearing cats, SR is predictive of tone-evoked thresholds (Kiang et al., 1965; Liberman and Kiang, 1978; Evans and Palmer, 1980). In cats with noise-induced hair cell damage, single unit recordings from auditory nerve fibers originating from the damaged region revealed that only a small percentage maintained low levels of spontaneous activity, whereas most fibers were unresponsive to acoustic stimulation and exhibited no SR whatsoever (Lieberman and Kiang, 1978; Liberman and Dodds, 1984a). In squirrel monkeys deafened by Kanamycin, spontaneous activity in the auditory nerve was completely abolished (Parkins, 1989). Selective abolition of inner hair cells also resulted in loss of SR in auditory nerve fibers in chinchillas (Wang et al., 1997). Collectively, the data indicate that a loss of spontaneous discharges in the auditory nerve is associated with inner hair cell injury.

In our sample of white cats, varying degrees of congenital deafness were expressed, and high SR did not predict low thresholds for acoustic activation. All auditory nerve fibers had high acoustic thresholds or were acoustically unresponsive irrespective of their SR. In completely deaf white cats, a few auditory nerve fibers (as defined by their presence in the auditory nerve) surprisingly exhibited low levels of spontaneous activity. The origin of spontaneous activity in normal cats is thought to arise from the stochastic release of transmitter from the hair cell (Furukawa and Ishii, 1967; Kiang et al., 1976; Furukawa et al., 1978). In this genetic model of auditory system degeneration, it remains to be determined how hair cell abnormalities exert their effects on auditory nerve activity or how auditory nerve fibers can have spontaneous discharges in the absence of receptor hair cells.

Activity and structure

Spike discharges in auditory nerve fibers clearly exert a substantial influence on cellular and synaptic morphology. For example, conductive and sensorineural hearing losses produce markedly different effects on target cell size (Pasic et al., 1994), and central structural alterations are tied to the cessation of spontaneous activity in sensorineural hearing loss as inferred from multiunit recordings (Tucci et al., 1987). Endbulb morphology is distinctly related to fiber activity in normal-hearing cats, where those of low SR fibers exhibit smaller but highly complex arborizations in comparison to those of high SR fibers (Sento and Ryugo, 1989). In the partially deaf white cats exhibiting both spontaneous discharges and sound-evoked spike activity, analysis revealed endbulbs to be intermediate in size and complexity when compared to totally deaf white cats and pigmented cats with normal hearing. It appears that endbulb size and arborization complexity correspond to overall hearing sensitivity rather than to fiber SR.

Fig. 11. Electron micrographs of representative endbulbs from normal, partially deaf, and totally deaf cats. The endbulb synapses from cats with normal hearing exhibit the characteristic convex postsynaptic densities (PSDs) with synaptic vesicles filling the presynaptic ending. Those synapses from partially hearing cats have normal-appearing PSDs but an elevated accumulation of slightly smaller synaptic vesicles. Synapses from totally deaf cats are markedly abnormal; there are almost no synaptic vesicles in the presynaptic endbulb, and the PSDs are thickened and noticeably larger than normal. PSDs are indicated by arrowheads. EB, endbulb; SBC, spherical bushy cell.

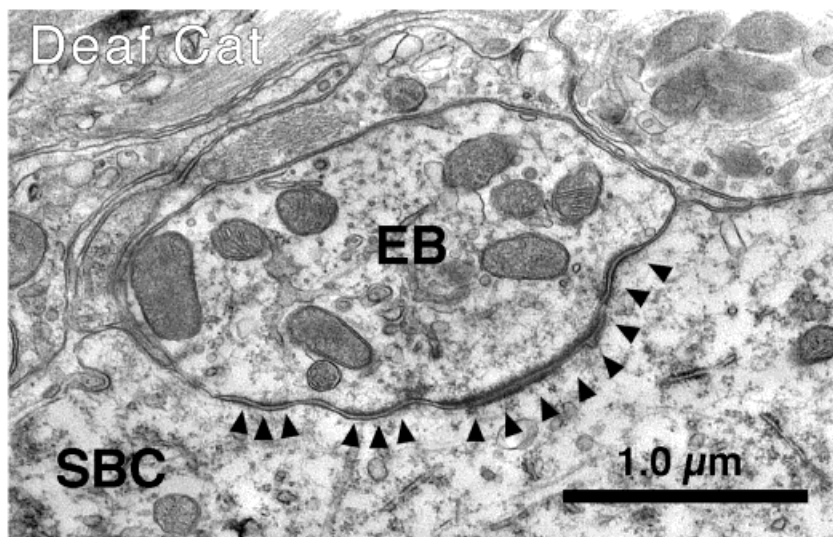
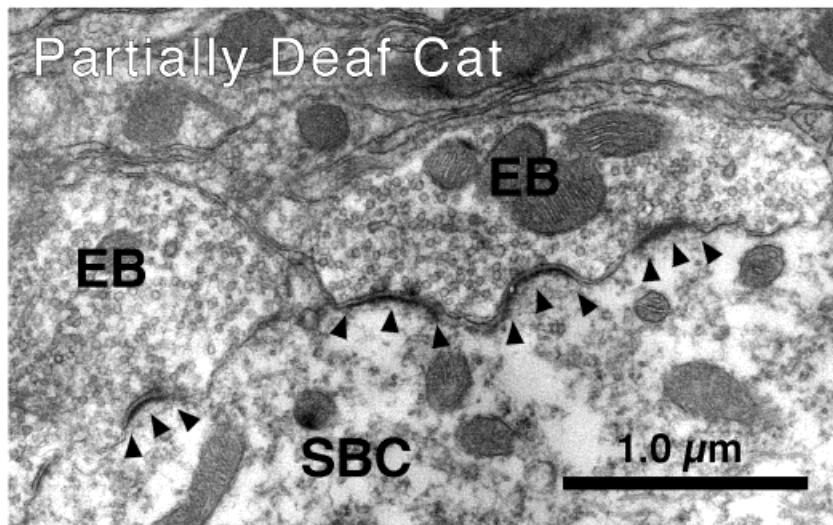
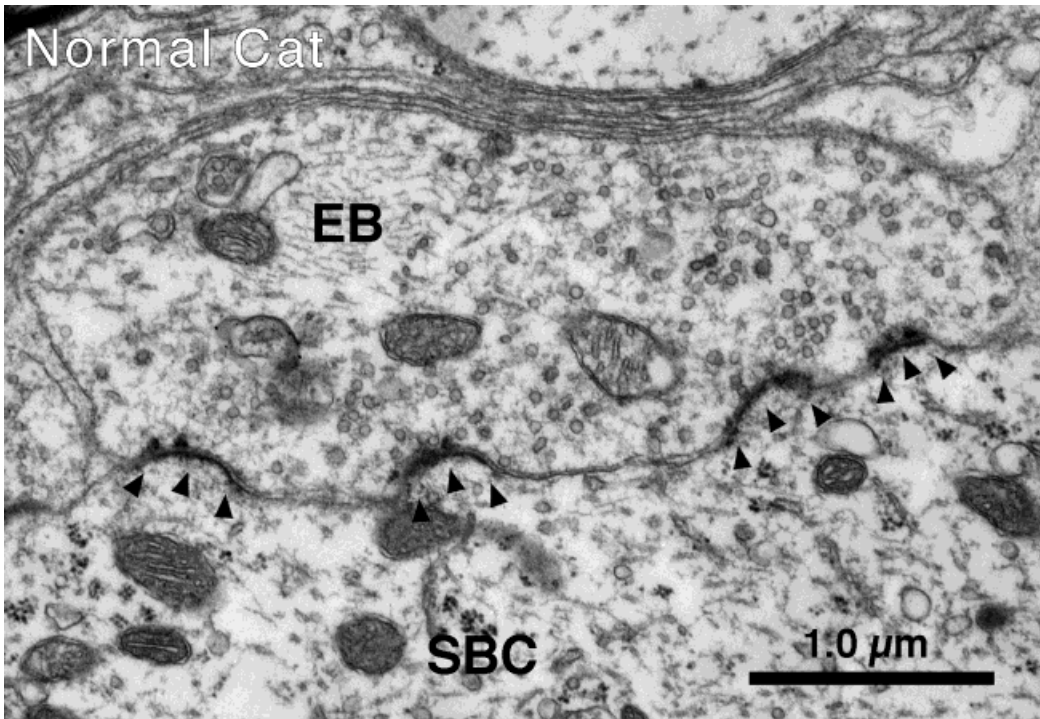


Figure 11

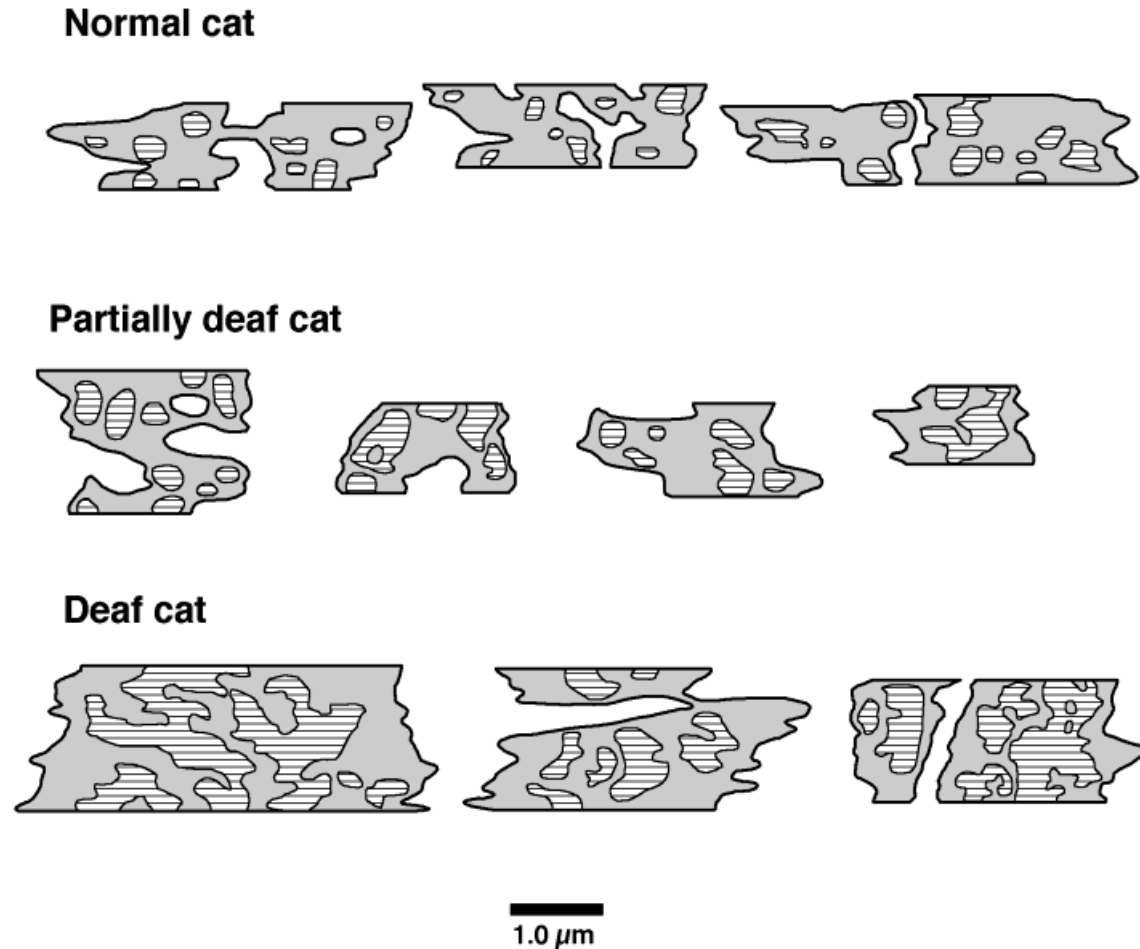


Fig. 12. Reconstructions of PSDs through serial-section electron microscopy and rotated to be viewed "en face." In other words, we are viewing the apposing membrane surface of spherical bushy cells that lies beneath the presynaptic endbulb. The reconstructions are representative for the different groups of cats. Apposition membrane is

shaded gray, and PSDs have line intervals equivalent to the thickness of the ultrathin sections. Normal cats have small PSDs with relatively regular shapes. Those of partially deaf cats are slightly larger (but not statistically so, $P = .09$), whereas those of totally deaf cats are largest compared to either of the other groups of endbulbs ($P < .05$).

The general level of presynaptic neuronal activity in endbulbs seems to exert a detectable effect upon the postsynaptic spherical bushy cell. In normal-hearing cats, spherical bushy cells postsynaptic to endbulbs of low SR fibers are smaller than those postsynaptic to endbulbs of high SR fibers (Sento and Ryugo, 1989). In congenitally DWCs, spherical bushy cells are smaller in size compared to those in pDWCs, and both are smaller when compared to those in normal cats (West and Harrison, 1973; Larsen and Kirchhoff, 1992; Saada et al., 1996). Also in the DWCs, synapses between auditory nerve fibers and spherical bushy cells are strikingly altered: There is a severe reduction of synaptic vesicles in the presynaptic ending and a striking expansion of postsynaptic densities (Ryugo et al., 1997).

The nature of the signal that mediates these graded changes in pre- and postsynaptic morphology remains to be determined. It is evident that spontaneous activity is not the defining variable in DWCs that mediates structure-function relationships. There is a relationship between cochlear structure, hearing thresholds (as indicated by single unit evoked activity), endbulb morphology, and

synapse structure. Recall that spontaneous discharges in auditory nerve fibers are independent and random events (Kiang et al., 1965; Walsh et al., 1972). Suprathreshold acoustic stimulation, however, will synchronize both excitatory and inhibitory activity with other crucial (but as yet unknown) events which could serve to stabilize endbulb structure. Presumably, the randomly occurring spontaneous discharges are not sufficient to initiate the necessary chain of events. Consistent with our observations is the idea that synchronous patterning of spike activity is important in governing the formation of normal connections (e.g., Shatz, 1990; Goodman and Shatz, 1993).

Functional implications

Morphological evaluation of temporal bones revealed that in the totally deaf white cats, there was no organ of Corti remaining and the number of spiral ganglion cells was reduced by more than 90% compared to normal-hearing cats. In those white cats having elevated hearing thresholds, the main elements in the cochlear duct were present but not necessarily normal. There was also evidence of endolymphatic hydrops, an abnormally small

tectorial membrane, hypertrophy of supporting cells, and a reduction in the number of spiral ganglion neurons. It is of particular interest that in the totally deaf white cats, Reissner's membrane is collapsed, as if endolymphatic volume had dropped. In the partially deaf cats, it appeared as if endolymphatic volume had increased, and oscillations of endolymphatic volume were suggested in deaf white cats to account for the different appearance of Reissner's membrane in histologic preparations (Bosher and Hallpike, 1965). Because lowering the endolymphatic pressure produces a decrease in the spontaneous discharge rates of auditory nerve fibers (Sewell, 1984), it would be useful to know if an increase in endolymphatic pressure produces a corresponding increase in spontaneous discharges.

This picture of various stages of cochlear degeneration has been described in hereditary (Fisch, 1959) and acquired (Schuknecht, 1993) deafness in humans, as well as in congenitally deaf white cats (Suga and Hattler, 1970; Bergsma and Brown, 1971; Mair, 1973; Rebillard et al., 1976). Degeneration of spiral ganglion cells had been considered an invariant histopathological consequence of profound sensorineural deafness that begins with hair cell loss (Mair, 1973; Otte et al., 1978), but as others have reported, spiral ganglion neuron loss is evident even if there is some hearing ability and without a mandatory preceding loss of hair cells (Rebillard et al., 1976, 1981a,b; Pujol et al., 1977; Leake et al., 1997). The mere presence of sensory structures, however, does not necessarily indicate that the structures have retained their normal function. Because the magnitude of spiral ganglion cell loss likely affects information transfer to the auditory pathways, it is important to identify all factors and influences that impact upon the status of the auditory nerve.

Clinical implications

The rationale for augmentation strategies for humans with hearing deficits is to restore neuronal responsivity to the auditory system. The type of intervention, whether in the form of hearing aids or cochlear implants, requires that neuronal populations of the ascending pathways respond in reliable and systematically predictable patterns to defined inputs and are able to transmit their responses in an organized way to the next synaptic station. In profoundly deaf humans, "simulated" acoustic input can be delivered to the central auditory system via cochlear implants which bypass the nonfunctioning cochlea. Multichannel cochlear implants can provide intensity-, temporal-, and spectral-based cues, and with intact central processing, should yield "cognitive hearing." Synaptic alterations at any site along this pathway, however, could severely corrupt the transmission of information from one level to the next. The cochlear nucleus, then, not only represents a key synaptic station whose integrity is required for the coherent transmission of acoustic information into the brain, but also is vulnerable to pathology induced by sensory deprivation.

We recently demonstrated that 6 or more months of congenital deafness exert a prominent influence on endbulb morphology and synaptic structure (Ryugo et al., 1997). In the present study, the size and complexity of the endbulbs were correlated with levels of evoked activity in the auditory nerve and the structural status of the organ of Corti. The severity of the hearing loss as assessed by electrophysiological recording methods and reflected in the histopathology of the organ of Corti seems to be linked

to endbulb appearance. The profoundly deaf cats with little neural activity exhibited endbulbs having the most compromised form. Those cats with some hearing but at elevated thresholds (and by inference with much less overall activity in auditory neurons) exhibited endbulbs and synapses that appeared almost normal. Although these endbulbs were still structurally distinguishable from those of normal-hearing cats, the data nevertheless suggest that some amount of hearing, or at least some sound-evoked responses, are important in stabilizing endbulb development and synapse formation. Perhaps the condition of the auditory system in partially deaf cats resembles that of postlingually deafened humans in that the auditory system has been preserved by function. Greater preservation of the auditory system may explain the greater benefits in some patients with cochlear implants. These kinds of data may contribute to treatment strategies for congenitally deaf individuals as well as to the development of more rational criteria in candidate selection for cochlear implants (Gantz et al., 1994; Waltzman et al., 1994).

ACKNOWLEDGMENTS

The authors gratefully thank Edward S. Aboujaoude and Tan Pongstaporn for technical assistance and Charles J. Limb and John R. Doucet for critical reading of the manuscript. We also thank Roger L. Miller, John R. Schilling, Kevin R. Franck, and Eric D. Young for sharing Q₁₀ data used in Figure 4. Portions of these results were presented in abstract form at the Eighteenth Midwinter Research Meeting of the Association for Research in Otolaryngology, St. Petersburg Beach, FL, February 5-9, 1995.

LITERATURE CITED

- Abercrombie, M. (1946) Estimation of nuclear population from microtome sections. *Anat. Rec.* 94:239-247.
- Bergsma, D. and K. Brown (1971) White fur, blue eyes, and deafness in the domestic cat. *J. Hered.* 62:171-185.
- Born, D.E. and E.W. Rubel (1985) Afferent influences on brain stem auditory nuclei of the chicken: neuron number and size following cochlea removal. *J. Comp. Neurol.* 231:435-445.
- Bosher, S. and C. Hallpike (1965) Observations on the histological features, development and pathogenesis of the inner ear degeneration of the deaf white cat. *Proc. R. Soc. Lond. [Biol.]* 162:147-170.
- Bourk, T.R., J.P. Mielcarz, and B.E. Norris (1981) Tonotopic organization of the anteroventral cochlear nucleus of the cat. *Hearing Res.* 4:215-241.
- Deol, M.S. (1970) The relationship between abnormalities of pigmentation and of the inner ear. *Proc. R. Soc. Lond. [Biol.]* 175:201-217.
- Evans, E.F. and A.R. Palmer (1980) Relationship between the dynamic range of cochlear nerve fibers and their spontaneous activity. *Exp. Brain Res.* 40:115-118.
- Fekete, D.M., E.M. Rouiller, M.C. Liberman, and D.K. Ryugo (1984) The central projections of intracellularly labeled auditory nerve fibers in cats. *J. Comp. Neurol.* 229:432-450.
- Fisch, L. (1959) Deafness as part of an hereditary syndrome. *J. Laryngol. Otol.* 73:355-383.
- Furukawa, T. and Y. Ishii (1967) Neurophysiological studies of hearing in goldfish. *J. Neurophysiol.* 30:1377-1403.
- Furukawa, T., Y. Hayashida, and S. Matsuura (1978) Quantal analysis of the size of excitatory post-synaptic potentials at synapses between hair cells and afferent nerve fibres in goldfish. *J. Physiol. (Lond.)* 276:211-226.
- Gantz, B.R., Tyler, G. Woodworth, N. Tye-Murray, and H. Fryauf-Bertschy (1994) Results of multichannel cochlear implants in congenital and acquired prelingual deafness in children: five year follow up. *Am. J. Otol.* 15:1-8.

- Goodman, C.S. and C.J. Shatz (1993) Developmental mechanisms that generate precise patterns of neuronal connectivity. *Cell* 72:77–98.
- Hartmann, R., G. Topp, and R. Klinke (1984) Discharge patterns of the domestic cat primary auditory fibers with electrical stimulation of the cochlea. *Hearing Res.* 19:85–88.
- Huchton, D.M., T. Pongstaporn, J.K. Niparko, and D.K. Ryugo (1997) Ultrastructural features of endbulbs of Held in deaf white cats. *Otolaryngol. Head Neck Surg.* 116:286–293.
- Keithley, E.M. and R.C. Schreiber (1987) Frequency map of the spiral ganglion in the cat. *J. Acoust. Soc. Am.* 81:1036–1042.
- Kiang, N.Y.S., T. Watanabe, L.C. Thomas, and L.F. Clark (1965) *Discharge Patterns of Single Unit Fibers in the Cat's Auditory Nerve.* Cambridge: MIT Press.
- Kiang, N.Y.S., M.C. Liberman, and R.A. Levine (1976) Auditory nerve activity in cats exposed to ototoxic drugs and high intensity sounds. *Ann. Otol. Rhinol. Laryngol.* 85:752–769.
- Kiang, N.Y.S., W.F. Liberman, W.F. Sewell, and J.J. Guinan (1986) Single unit clues to cochlear mechanisms. *Hear. Res.* 22:171–182.
- Larsen, S.A. and T.M. Kirchhoff (1992) Anatomical evidence of plasticity in the cochlear nuclei of deaf white cats. *Exp. Neurol.* 115:151–157.
- Leake, P.A., A.L. Kuntz, C.M. Moore, and P.L. Chambers (1997) Cochlear pathology induced by aminoglycoside ototoxicity during postnatal maturation. *Hear. Res.* 113:117–132.
- Liberman, M.C. (1978) Auditory-nerve responses from cats raised in a low-noise chamber. *J. Acoust. Soc. Am.* 63:442–455.
- Liberman, M.C. (1982) The cochlear frequency map for the cat: labeling auditory-nerve fibers of known characteristic frequency. *J. Acoust. Soc. Am.* 75:1441–1449.
- Liberman, M.C. and L.W. Dodds (1984a) Single neuron labeling and chronic cochlear pathology. II. Stereocilia damage and alterations of spontaneous discharge rates. *Hearing Res.* 16:43–53.
- Liberman, M.C. and L.W. Dodds (1984b) Single neuron labeling and chronic cochlear pathology. III. Stereocilia damage and alterations of threshold tuning curves. *Hear. Res.* 16:55–74.
- Liberman, M.C. and N.Y.S. Kiang (1978) Acoustic trauma in cats. Cochlear pathology and auditory nerve activity. *Acta Otolaryngol.* 358:1–63.
- Lippe, W.R., O. Steward, and E.W. Rubel (1980) The effects of unilateral basilar papilla removal upon nuclei laminaris and magnocellularis of the chick examined with (3H) 2-deoxy-D-glucose autoradiography. *Brain Res.* 196:43–58.
- Lurie, M.H. (1948) The membranous labyrinth in the congenitally deaf collie and Dalmatian dog. *Laryngoscope* 58:279–287.
- Mair, I.W. (1973) Hereditary deafness in the white cat. *Acta. Otolaryngol.* 314:1–48.
- Mandelbrot, B.B. (1982) *The Fractal Geometry of Nature.* New York: W.H. Freeman.
- Niparko, J.K. and P. Finger (1977) Cochlear nucleus cell size changes in the Dalmatian: model of congenital deafness. *Otolaryngol. Head Neck Surg.* 17:229–235.
- Otte, J., H.F. Schuknecht, and A.G. Kerr (1978) Ganglion cell populations in the normal and pathological human cochleae. Implications for cochlear implantation. *Laryngoscope* 88:1231–1246.
- Parkins, C.W. (1989) Temporal response patterns of auditory nerve fibers to electrical stimulation in deafened squirrel monkeys. *Hear. Res.* 41:137–168.
- Pasic, T.R., D.R. Moore, and E.W. Rubel (1994) Effect of altered neuronal activity on cell size in the medial nucleus of the trapezoid body and ventral cochlear nucleus of the gerbil. *J. Comp. Neurol.* 348:111–120.
- Porter, R., S. Ghosh, G.D. Lange, and T.G. Smith, Jr. (1991) A fractal analysis of pyramidal neurons in mammalian motor cortex. *Neurosci. Lett.* 130:112–116.
- Pujol, R., M. Rebillard, and G. Rebillard (1977) Primary neural disorders in the deaf white cat cochlea. *Acta Otolaryngol.* 83:59–64.
- Rebillard, G., M. Rebillard, E. Carlier, and R. Pujol (1976) Histo-physiological relationships in the deaf white cat auditory system. *Acta Otolaryngol.* 82:48–56.
- Rebillard, M., R. Pujol, and G. Rebillard (1981a) Variability of the hereditary deafness in the white cat. II. Histology. *Hearing Res.* 5:189–200.
- Rebillard, M., G. Rebillard, and R. Pujol (1981b) Variability of the hereditary deafness in the white cat. I. Physiology. *Hearing Res.* 5:179–187.
- Rubel, E.W., R.L. Hyson, and D. Durham (1990) Afferent regulation of neurons in the brain stem auditory system. *J. Neurobiol.* 21:169–196.
- Ryugo, D.K. and S.K. May (1993) The projections of intracellularly labeled auditory nerve fibers to the dorsal cochlear nucleus of cats. *J. Comp. Neurol.* 329:20–35.
- Ryugo, D.K., M.M. Wu, and T. Pongstaporn (1996) Activity-related features of synapse morphology: a study of endbulbs of Held. *J. Comp. Neurol.* 365:141–158.
- Ryugo, D.K., T. Pongstaporn, D.M. Huchton, and J.K. Niparko (1997) Ultrastructural analysis of primary endings in deaf white cats: morphologic alterations in endbulbs of Held. *J. Comp. Neurol.* 385:230–244.
- Saada, A.A., J.K. Niparko, and D.K. Ryugo (1996) Morphological changes in the cochlear nucleus of congenitally deaf white cats. *Brain Res.* 736:315–328.
- Schuknecht, H.F. (1993) *Pathology of the Ear.* Philadelphia: Lea & Febiger.
- Schwartz, I.R. and J.F. Higa (1982) Correlated studies of the ear and brainstem in the deaf white cat: changes in the spiral ganglion and the medial superior olivary nucleus. *Acta Otolaryngol.* 93:9–18.
- Sento, S. and D.K. Ryugo (1989) Endbulbs of Held and spherical bushy cells in cats: Morphological correlates with physiological properties. *J. Comp. Neurol.* 280:553–562.
- Sewell, W.F. (1984) The relation between the endocochlear potential and spontaneous activity in auditory nerve fibres of the cat. *J. Physiol. (Lond.)* 347:685–696.
- Shatz, C.J. (1990) Impulse activity and the patterning of connections during CNS development. *Neuron* 5:745–756.
- Shone, G., Y. Raphael, and J.M. Miller (1991) Hereditary deafness occurring in CD/1 mice. *Hear. Res.* 57:153–156.
- Smith, T.G.J., W.B. Marks, G.D. Lange, and W.H.J. Sheriff (1989) A fractal analysis of cell images. *J. Neurosci.* 27:173–180.
- Suga, F. and K.W. Hattler (1970) Physiological and histopathological correlates of hereditary deafness in animals. *Laryngoscope* 80:81–104.
- Sugiura, A. and D.A. Hilding (1970) Cochleo-saccular degeneration in Hedlund mink. *Acta Otolaryngol.* 69:126–137.
- Tucci, D.L., D.E. Born, and E.W. Rubel (1987) Changes in spontaneous activity and CNS morphology associated with conductive and sensorineural hearing loss in chickens. *Ann. Otol. Rhinol. Laryngol.* 96:343–350.
- Walsh, B.J., J.B. Miller, R.R. Gacek, and N.Y.S. Kiang (1972) Spontaneous activity in the eighth cranial nerve of the cat. *Intern. J. Neurosci.* 3:221–236.
- Waltzman, S., S. Fisher, J.K. Niparko, and N. Cohen (1994) Predictors of postoperative performance with cochlear implants. *Ann. Otol. Rhinol. Laryngol.* 165:15–18.
- Wang, J., N.L. Powers, P. Hofstetter, P. Trautwein, D. Ding, and R. Salvi (1997) Effects of selective inner hair cell loss on auditory nerve fiber threshold, tuning and spontaneous and driven discharge rate. *Hear. Res.* 107:67–82.
- Weisleder, P. and T.J. Park (1994) Belgian Waterslager canaries are afflicted by Scheibe's-like dysplasia. *Hear. Res.* 80:64–70.
- West, C.D. and J.M. Harrison (1973) Transneuronal cell atrophy in the deaf white cat. *J. Comp. Neurol.* 151:377–398.
- Wilson, T.G. and F. Kane (1959) Congenital deafness in white cats. *Acta Otolaryngol.* 50:269–277.
- Wright, S. (1918) Color inheritance in mammals. *J. Hered.* 9:87–90.